Available online at www.sciencedirect.com
SCIENCE DIRECT®
ELSEVIER
Journal of Nuclear Materials 337–339 (2005) 386–390
journal of nuclear materials
www.elsevier.com/locate/jnucmat

Simple Core-SOL-Divertor model and its application to operational space of HT-7U

R. Hiwatari [a,*], Y. Kuzuyama [b], A. Hatayama [b], K. Okano [a], Y. Asaoka [a], S. Zhu [c], Y. Tomita [d]

[a] *Central Research Institute of Electric Power Industry, 2-11-1 Iwado Kita, Komae-shi, Tokyo 201-8511, Japan*
[b] *Faculty of Science and Technology, Keio University, Yokohama, Japan*
[c] *Institute of Plasma Physics, Chinese Academy of Sciences, Hefei, PR China*
[d] *National Institute for Fusion Science, Toki, Japan*

Abstract

We develop a simple Core-SOL-Divertor (C-S-D) model to investigate qualitatively the overall features of the operational space for the integrated core and edge plasma. To construct the simple C-S-D model, a simple core plasma model of ITER physics guidelines and a two-point SOL-divertor model are used. The simple C-S-D model is applied to the study of the HT-7U operational space with lower hybrid current drive experiments under various kinds of trade-off for the basic plasma parameters. Effective methods for extending the operation space are also presented. From this study for the HT-7U operation space, it is shown that the C-S-D model is a useful tool to understand qualitatively the overall features of the plasma operation space.

PACS: 28.52.Av; 52.55.Fa; 52.55.Rk
Keywords: Divertor modeling; Particle balance; Power balance; HT-7U

1. Introduction

Consistency between the edge plasma operation and the core plasma operation is an important issue for the design of ITER and the future fusion power plant. In case of the ITER divertor predictive modeling, the fitting scaling laws for divertor plasma property are built with a two dimensional (2D) divertor transport code, and these are used as boundary conditions for the core plasma analysis [1,2]. Prior to such detailed and massive calculations by multi-dimensional transport codes, it is useful to understand qualitatively the overall features of plasma operational space including the requirements for the SOL and divertor plasma. For this purpose, we are developing a simple Core-SOL-Divertor (C-S-D) model. The basic concept of the C-S-D model was presented in Ref. [3]. In the present paper, we improve the C-S-D model and apply it to investigate the plasma operational space of low hybrid current drive (LHCD) experiments for HT-7U.

* Corresponding author.
E-mail addresses: hiwatari@criepi.denken.or.jp (R. Hiwatari), akh@ppl.appi.keio.ac.jp (A. Hatayama).

0022-3115/$ - see front matter © 2004 Elsevier B.V. All rights reserved.
doi:10.1016/j.jnucmat.2004.10.043

2. Simple Core-SOL-Divertor model

2.1. Core plasma and SOL-divertor plasma model

We apply the 0D plasma model based on ITER physics guidelines to the core plasma transport [4]. The usual definitions for the global particle and power balance are applied in the present paper [3], and the particle and energy confinement times are required to solve 0D plasma transport model. The scaling law of the L-mode energy confinement time $\tau_E^{\rm ITER89L}$ [4] is applied to the energy confinement time $\tau_E = f_H \tau_E^{\rm ITER89L}$, where f_H (=2.0) is the confinement improvement factor for H-mode. The particle confinement time τ_p is defined by $\tau_p = C_p \tau_E$, where C_p is the correction factor for each species. In the present paper, $C_p = 1.0$ is assumed. The L–H transition condition is also installed by the same fashion as in Ref. [5], where the experimental scaling law [6] is applied to the threshold power.

The two-point model [7] under steady state conditions can be applied with a time dependent core transport model, because the time scale of core plasma transport is much longer than that of SOL-divertor plasma. Basic equations of the usual two-point model are as follows:

$$(1 - f_{\rm mom}^{\rm div}) n_s T_s = (1 + M_d^2) n_d T_d, \tag{1}$$

$$\frac{7}{2}(1 - f_{\rm imp}) L_s q_\perp = n_d M_d C_s(T_d) \Delta \left[\varepsilon + (\gamma + M_d^2) T_d\right], \tag{2}$$

$$\Delta = \frac{5}{2} \chi_\perp \frac{n_s T_s}{q_\perp}, \tag{3}$$

$$L_d^2 q_\perp = \frac{4\kappa_0 \Delta}{49} T_s^{7/2} \left[1 - \left(\frac{T_d}{T_s}\right)^{7/2}\right], \tag{4}$$

where n and T are density and temperature. The subscript 's' and 'd' express the upstream SOL and divertor region, respectively. The heat flux from the core plasma, temperature decay length, and Mach number at the divertor plate are defined by $q_\perp$, Δ, and M_d, respectively. The coefficients $f_{\rm mom}^{\rm div}$ and $f_{\rm imp}$ are the fraction of momentum loss and impurity radiation loss. The coefficient γ ($\approx$7.0) is the sheath energy transmission coefficient, and the heat load ε ($\approx$21.8 eV) on the plate comes from the recombination and radiation process [8].

2.2. Particle balance to determine the upstream SOL density

In order to integrate the core and edge plasma model, the upstream SOL density n_s should be given in a self-consistent manner both for the core plasma and for the edge plasma. For this purpose, the particle balance equation in the SOL and divertor regions is used. We assume that all neutral particles originate at the divertor plate at the rate proportional to the total particle flux to the divertor plate. Consequently, total neutral source rate at the edge region N_n including gas puff term $N_{\rm puff}$ is as follows:

$$N_n = \frac{1}{2}\left(1 - \frac{1}{e^2}\right) n_d M_d C_s 2\pi R \Delta_n \sin(\psi) + N_{\rm puff}, \tag{5}$$

where Δ_n is the density decay length. We assume that $\Delta_n = 2\Delta$. ψ is the angle of the magnetic field to the divertor plate. The term $(1/2)(1 - 1/e^2)$ comes from the integration of the radial direction (from the separatrix to the density decay length Δ_n) on the divertor plate. By using the simple neutral model and the particle flux across the separatrix, $\Gamma_{\rm core}$, from the 0D core plasma calculation, the particle balance equation for the SOL-divertor region becomes

$$\Gamma_{\rm core} S_{\rm core} + N_n^{\rm sol} + N_n^{\rm div} = \frac{1}{2}\left(1 - \frac{1}{e^2}\right) n_d M_d C_s 2\pi R \Delta_n \sin(\psi), \tag{6}$$

where $N_n^{\rm div} = f_{\rm ion}^{\rm div} N_n$ and $N_n^{\rm sol} = f_{\rm ion}^{\rm sol}(1 - f_{\rm ion}^{\rm div}) N_n$. $f_{\rm ion}^{\rm div}$ and $f_{\rm ion}^{\rm sol}$ are the ionization fraction in the divertor and the SOL region, respectively. $S_{\rm core}$ is the core plasma surface normal to the particle flux. The ionization fraction in the divertor region, which was not included in the previous study [3], is modeled by [9]

$$f_{\rm ion}^{\rm div} = 1 - \exp\left(-\frac{L_d \sin(\psi)}{\lambda_{\rm ion}^{\rm div}}\right), \tag{7}$$

where $\lambda_{\rm ion}^{\rm div} = v_n / (n_d \langle \sigma v \rangle_{\rm ion})$ is defined by the ionization cross section $\langle \sigma v \rangle_{\rm ion}$, which is the strong function of T_d, and the neutral velocity $v_n = \sqrt{T_n/m}$. In the present paper, the constant neutral temperature $T_n = 3$ eV is assumed. The ionization fraction in the SOL region is defined by

$$f_{\rm ion}^{\rm sol} = \frac{A_{\rm sol}}{A_{\rm core} + A_{\rm sol} + A_{\rm pump}}, \tag{8}$$

where $A_{\rm core}$, $A_{\rm sol}$ and $A_{\rm pump}$ are the effective areas for the core region, the SOL region, and the pumping effect from the divertor region, respectively. In the present paper, the effective areas of $A_{\rm core}$ and $A_{\rm sol}$ are assumed by the each cross section area on the plasma midplane, i.e., $A_{\rm core} = 2\pi R \cdot a$ and $A_{\rm sol} = 2\pi R \cdot \Delta_n$. The effective area of $A_{\rm pump}$ is defined by $A_{\rm pump} = C_{\rm pump}/(v_n/4)$, where $C_{\rm pump}$ is the speed of the pumping system [10], but pumping effect is not considered in the present paper ($C_{\rm pump} = 0.0$). To specify these parameters more precisely, numerical analysis by multi-dimensional Monte Calro neutral transport code will be done in the future.

To check the validity of this C-S-D model, comparison with the edge transport code (B2-EIRENE) is carried out. We focused on the JT-60U L-mode discharge in the high recycling state (Table 1) [11]. The density

Table 1
Main plasma parameters of JT-60U [11] and HT-7U [13]

	JT-60U	HT-7U
R/a (m)	3.4/0.8	1.97/0.5
κ_{95}/δ_{95} (–)	1.5/0.5	1.6/0.8
B_t (T)	3.5	3.5
I_p (MA)	1.8	1
P_{LHCD}/P_{aux} (MW)	–/–	3.5/7.5
Q_{in} (MW)	2.5	–
L_s/L_d (m)	50/3.0	31/4.3
f_{imp} (–)	0.3	0.3

and temperature of divertor-SOL region against the total particle flux across the separatrix Φ_p are shown in Fig. 1(a) and (b), where superscripts of 'CSD' and 'B2' corresponds C-S-D model and B2-EIRENE code, respectively. Qualitatively, the result of the C-S-D model is similar to that of B2-EIRENE. Quantitatively, the difference of temperature becomes large over $\Phi_p = 1.5 \times 10^{22}$ s^{-1}, mainly because B2-EIRENE result corresponds to the detached plasma state, which is not considered in the present C-S-D model. On the other hand, when n_s^{CSD} is equal to n_s^{B2} at about $\Phi_p = 1.3 \times 10^{22}$ s^{-1}, other parameters of the C-S-D model are also similar to those of B2-EIRENE. From this comparison, it is shown that the results by the C-S-D model are reasonable in qualitative sense. Around $\Phi_p = 1.0 \times 10^{22}$ s^{-1} density of the C-S-D model suddenly increases in Fig. 1(a) and temperature decreases sharply

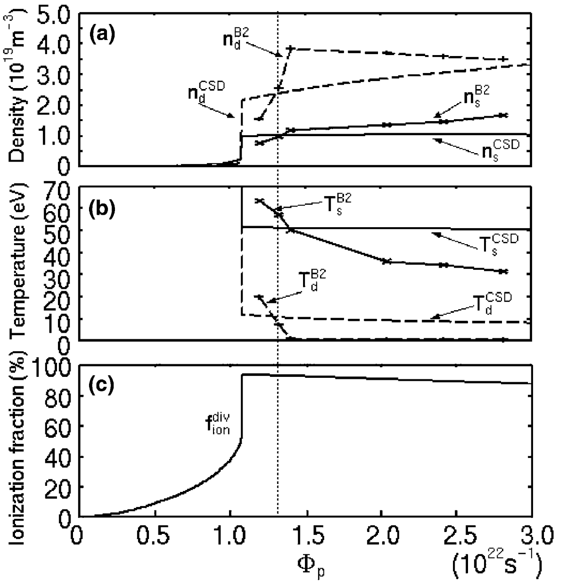

Fig. 1. The SOL-divertor parameters vs. the total particle flux Φ_p: (a) density, (b) temperature by the C-S-D model and the B2-EIRENE, and (c) is the ionization fraction in the divertor region by the C-S-D model.

in Fig. 1(b), which is considered to be the transition from low to high recycling state [12]. That transition is confirmed by the sudden increase of the ionization fraction in the divertor region by the C-S-D model (Fig. 1(c)). The further quantitative validation of the C-S-D model including the low to high recycling phenomena remains to be done.

3. HT-7U fully non-inductive operation space by low hybrid current drive

3.1. Main trade-off for the operation space

In the initial phase of the HT-7U plan, current drive experiments are planned to be carried out by LHCD [13]. Low density operation is preferable for good current drive efficiency. On the other hand, such operation is disadvantageous to the divertor performance, because it generally results in high heat load on the divertor plates. As for the steady state experiment with high performance plasma such as H-mode, reduction of the heat load onto the divertor plate is a critical issue. Considering discussions above, we take into account the following trade-off, or constraints, i.e., (1) available LHCD power, (2) allowable heat load to the divertor plates, (3) available heating power for sustaining the steady state power balance in the core and also (4) threshold power for L–H transition.

Based on the particle and power balance of the core plasma [3,4], the total particle flux Φ_p and the total heat flux Q_{in} across the separatrix are $\Phi_p = (n_{20}V_p)/(C_p\tau_E)$ and $Q_{in} = (0.048 n_{20} T V_p)/\tau_E$, respectively ($V_p$ is the plasma volume). From these quantities and the definition of the energy confinement time, the temperature and the density of the core plasma are written as $T = C_T Q_{in}/\Phi_p$ and $n_{20} = C_n \Phi_p^{10/9}/Q_{in}^{5/9}$, respectively (where C_T and C_n are functions of core plasma parameters). With these equations, we express the following trade-off, or constraints as functions of (Q_{in}, Φ_p), and discuss the plasma operation space on (Q_{in}, Φ_p).

The power required for LHCD is estimated by the following model [14]:

$$P_{LHCD} = \frac{R \ln \Lambda I_p}{0.122(j^*/p^*)} \frac{n_{20}}{T}. \tag{9}$$

The available LHCD power and plasma current I_p in Eq. (9) are set to be 3.5 MW and 1.0 MA for the HT-7U [13]. Then, Eq. (9) is written as

$$\frac{R \ln \Lambda}{0.122(j^*/p^*)} C_n \Phi_n^{19/9} C_T^{-1} Q_{in}^{-14/9} \leqslant 3.5, \tag{10}$$

where $(j^*/p^*) = 10$ is assumed in the present paper. In addition, the total heating power for the HT-7U is set to be 7.5 MW [13], then the following relationship has to be considered:

$$P_{\mathrm{LHCD}} \leqslant Q_{\mathrm{in}} \leqslant 7.5. \quad (11)$$

The left inequality in Eq. (11) is rewritten as

$$Q_{\mathrm{in}}^{23/19} \leqslant \frac{R \ln \Lambda I_{\mathrm{p}}}{0.122(j^*/p^*)} \frac{C_{\mathrm{n}}}{C_{\mathrm{T}}} \Phi_{\mathrm{p}}^{19/9}. \quad (12)$$

The scaling law of the threshold power for the L–H transition can be also written as the function of Φ_{p} and Q_{in},

$$Q_{\mathrm{in}} \geqslant P_{\mathrm{thr}} = 2.75 B_{\mathrm{t}}^{0.96} R^{1.23} a^{0.76} M_{\mathrm{i}}^{-1} C_{\mathrm{n}}^{0.77} \left(\frac{\Phi_{\mathrm{p}}^{7.7}}{Q_{\mathrm{in}}^{3.85}} \right)^{1/9}, \quad (13)$$

where M_{i} is the average ion mass (amu). The heat flux q_{div} to the divertor plates is limited to the maximum allowable heat flux q_{max} from the engineering viewpoint. This condition is expressed as

$$q_{\mathrm{div}} = \lfloor \varepsilon + (\gamma + M_{\mathrm{d}}^2) T_{\mathrm{d}} \rfloor n_{\mathrm{d}} M_{\mathrm{d}} C_{\mathrm{s}} \sin(\psi) \sin(\theta) \leqslant q_{\mathrm{max}}, \quad (14)$$

where θ denotes the inclination angle of the divertor plate to the magnetic lines force in the poloidal plane. Eq. (14) also can be expressed by Φ_{p} and Q_{in} defined above. The q_{max} is taken to be 3.5 MW/m^2, which corresponds to the averaged value estimated in Ref. [13]. Finally, we obtain the four inequalities, i.e, Eqs. (10), (12)–(14), for the trade-off relationships of LHCD experiments.

3.2. Basic and qualitative features for HT-7U operational space

The main parameters of HT-7U are summarized in Table 1 [13]. With these parameters, we explore the possible operation space in the (Q_{in}, Φ_{p}) space as shown in Fig. 2. The operational space is painted, and each boundary is the operation condition as mentioned in the previous subsection. Fig. 2 indicates that the allowable heat flux to the divertor plate is a key parameter to extend the possible operation space. The upper boundary of Q_{in} is limited to 3.0 − 3.5 MW by $q_{\mathrm{div}} \leqslant 3.5$ MW/m^2. The boundary of $q_{\mathrm{div}} \leqslant 3.5$ MW/m^2 for $Q_{\mathrm{in}} \leqslant 3.0$ MW region implies a decrease of q_{div} by the transition from low to high recycling state. The upper boundary of the particle flux Φ_{p} is dominated by the power balance requirement for the low Q_{in} region, while it is limited by the available LHCD power for higher Q_{in}. In other words, the available power for the LHCD tends to be a key parameter to extend the operation density of the core plasma in this high Q_{in} regime. In this exploration, no gas puffing in the divertor region is assumed. The sudden changes of the curve for the required LHCD power and the power balance around (Q_{in}, Φ_{p}) ≈ (1.5 MW, 1.5×10^{21} s^{-1}) are caused by the L–H transition.

To extend the operational space, the following methods have been investigated in the qualitative sense. In this series of investigation, the remaining parameters except the key parameter in the following methods are kept at the same values as those in Fig. 2. To extend the operational space, the divertor temperature has to be reduced. Gas puffing in the edge region is one of the candidates for the decrease of the divertor temperature. When $N_{\mathrm{puff}} = 1.0 \times 10^{21}$ s^{-1} (which corresponds to about 5% of total neutral source rate N_{n}) is fuelled in the divertor region, the operational space is extended toward both the lower particle flux range of $\Phi_{\mathrm{p}} \approx 1.0 \times 10^{21}$ s^{-1} and the higher heat flux range of $Q_{\mathrm{in}} = 3.3 - 4.0$ MW (Fig. 3(a)). The impurity seeding in the SOL-divertor region is also one of the candidates to extend the operation boundary. When it is possible to increase up to $f_{\mathrm{imp}} = 0.6$ of the impurity radiation loss

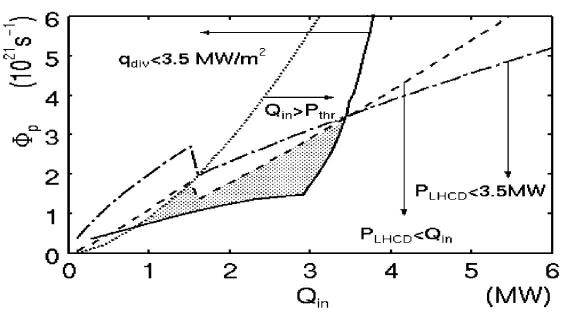

Fig. 2. Qualitative features of HT-7U operational space.

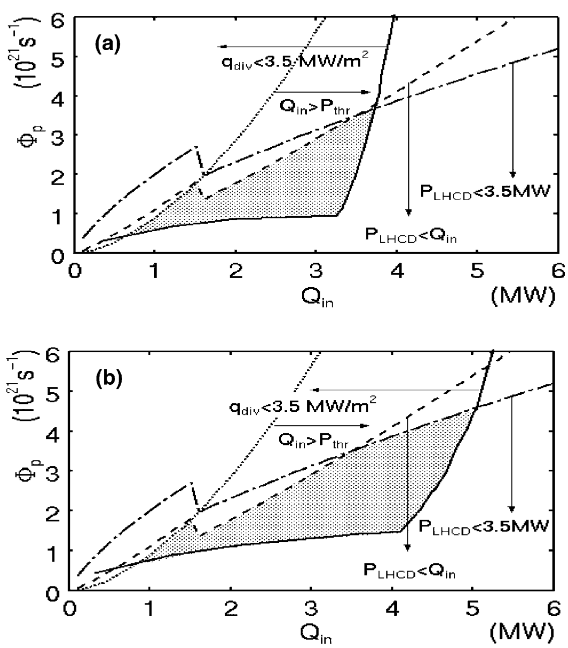

Fig. 3. The effect on gas puffing (a) and the impurity seeding (b) on the HT-7U operational space.

fraction similar to the ITER divertor design, then the upper boundary of Q_{in} is extended up to $Q_{in} \approx 5.0$ MW (Fig. 3(b)). Of course, the impact of the impurity seeding on core plasma performance should be carefully checked by the more detailed numerical simulations, because f_{imp} is given as the input parameter in the C-S-D model. In addition, the effect of impurity seeding on the efficiency of LHCD is not calculated, either. By using the C-S-D model, it is revealed that gas puffing is an effective method to extend the operational space toward both lower Φ_p and higher Q_{in} region. On the other hand, achievement of $f_{imp} = 0.6$ has the possibility to extend up to $Q_{in} \approx 5.0$ MW region.

4. Summary

The C-S-D model has been developed to investigate overall and integrated features of core and edge plasma in tokamaks, and applied to the analysis of the HT-7U operational space. The basic features of possible operational space have been studied for the LHCD steady-state operation. Various kinds of trade-off have been taken account into in the analysis. Furthermore, we have confirmed that gas puffing and impurity seeding in the edge region have the potential to extend the operational space. From these applications to the study of the HT-7U operation space, the C-S-D model is shown to be a useful tool to understand qualitatively the overall features of the operational space for future reactors under various kinds of trade-off. Of course, the quantitative validation of the particle transport including the low to high recycling state transition in the C-S-D model remains to be done because of the simple model such as the neutral transport model mentioned in Section 2.2.

Acknowledgments

The authors gratefully acknowledge stimulating discussions with T. Takizuka and N. Hayashi in JAERI. The authors also would like to thank Y. Ogawa of the University of Tokyo for his helpful comments on this study. This work is partly supported by JSPS-CAS Core-University Program on Plasma and Nuclear Fusion.

References

[1] A.S. Kukushkin et al., IAEA-CN77/CT/P-07, in: G.W. Pacher (Ed.), Proceedings of the 19th IAEA Fusion Energy Conference, Lyon, France, 2002.
[2] G.W. Pacher et al., Nucl. Fus. 43 (2003) 188.
[3] R. Hiwatari et al., Contrib. Plasma Phys. 44 (2004) 76.
[4] N. Uckan, ITER Physics Group 1990 ITER Physics Design Guidelines:1989, ITER Documentation Series No. 10.
[5] T. Yamamoto et al., Fusion Eng. Des. 39&40 (1998) 143.
[6] ITER Physics Expert Groups on Confinement and Transport and Confinement Modeling and Database, ITER Physics Basis Editors, Nucl. Fus. 39 (1999) 2175.
[7] K. Borrass, Nucl. Fus. 31 (1991) 1035.
[8] S. Takamura, J. Plasma Fus. Res. 72 (1996) 866 (in Japanese).
[9] N. Hayashi et al., J. Phys. Soc. Jpn. 66 (1997) 3815.
[10] M. Sugihara et al., J. Nucl. Mater. 241–243 (1997) 299.
[11] A. Hatayama et al., Nucl. Fus. 40 (2000) 2009; J. Nucl. Mater. 290–293 (2001) 407.
[12] M. Sugihara et al., J. Nucl. Mater. 128&129 (1984) 114.
[13] S. Zhu, Contrib. Plasma Phys. 40 (2000) 322.
[14] S. Takamura, Purazuma Kanetsu Kisoron, Nagoya Daigaku Shuppankai, 1986 (in Japanese).